Olexander Glotka, Olexander Mityayev, Valeriy Netrebko, Oleksandr Petrashov*

NATURE OF CYCLIC DESTRUCTION OF ALUMINIUM ALLOY FOR ENGINE PISTONS

PRIRODA RAZARANJA ZAMOROM LEGURE ALUMINIJUMA ZA KLIPOVE MOTORA

Originalni naučni rad / Original scientific paper
Rad primljen / Paper received: 29.05.2024
https://doi.org/10.69644/ivk-2025-03-0461

Adresa autora / Author's address:
Zaporizhzhia Polytechnic National University, Zaporizhzhia, Ukraine, *email: Glotka-alexander@ukr.net
O. Glotka https://orcid.org/0000-0002-3117-2687
O. Mityayev https://orcid.org/0000-0001-9034-1359
V. Netrebko https://orcid.org/0000-0003-3283-0116

Keywords
- aluminium alloy
- modification
- laser processing
- cyclic destruction

Ključne reči
- aluminijumska legura
- modifikacija
- laserska obrada
- ciklično

Abstract

The use of secondary materials in the modern world is one of the tasks that has a high priority. One of the harmful impurities in aluminium alloys is iron. Iron is included in the composition as an elongated intermetallic that significantly reduces the properties of the material. In this work, the effect of modification and laser processing on the processes of cyclic destruction of piston aluminium alloy AL25 at temperatures of 20 and 300 °C is considered. The effect of modification on the destruction processes of the secondary aluminium alloy is determined. Phases that reduce the fatigue strength of the alloy have been identified. The effect of laser processing of this material is analysed.

Izvod

Upotreba sekundarnih materijala (sirovina) u modernom svetu ima veliki prioritet. Jedna od štetnih nečistoća u legurama aluminijuma je železo. Železo se nalazi u sastavu kao izduženo intermetalno jedinjenje, koje u značajnoj meri slabi karakteristike materijala. U ovom radu se razmatra uticaj modifikacija i laserske obrade na procese razaranja usled zamora legure aluminijuma AL25 za klipove, na temperaturama 20 i 300 °C. Razmatraju se efekti modifikacije na proces razaranja sekundarne legure aluminijuma. Identifikuju se faze koje smanjuju zamornu čvrstoću legure. Analizira se i uticaj laserske obrade ovog materijala.

INTRODUCTION

Heat-resistant aluminium alloys (silumin) are used for the manufacture of parts operating at temperatures from 130 to 300 °C; parts include pistons, cylinder heads, discs and vanes of compressors of gas turbine engines /1-9/. At the moment, the casting alloy of the eutectic composition Al-12Si-2Cu-Mg-Ni (AK12M2MgN, AL25) has become the most widely used for the manufacture of pistons. The advantages of this alloy are low density, high strength and thermal conductivity, low temperature coefficient of linear expansion and a high level of casting properties, /10-16/.

Due to the accumulation of a large amount of production waste (spouts, fumes, lack of parts, shavings, remelting of waste and splashes, and used parts), an urgent task has arisen in the use of this type of material. However, repeated remelting reveals that due to the introduction of various impurities into the charge, primarily iron, the formation of complex intermetallic of plate shape and large sizes is possible which significantly reduces the level of mechanical and operational properties of aluminium alloys. To eliminate the harmful effects of intermetallic, their shape and size are changed with the help of modifying complexes, /17-20/.

Laser treatment is also a promising surface treatment to increase the durability of parts. When using this method, the material's physical, chemical, and mechanical properties significantly increase, /21-24/.

The purpose of the work is to study the processes of destruction under the action of cyclic loads of the secondary piston aluminium alloy AK12M2MgN (AL25), modified and additionally laser-treated.

METHODS OF RESEARCH

For the manufacture of the AK12M2MgN (AL25) alloy, 100 % of the production return is used which is cleaned of traces of corrosion, sand and scorch. In an electric resistance furnace using a cast iron crucible lined with graphite, 8 melts are melted, which subsequently underwent various types of processing (Table 1). All melts are treated with coating flux (33 mass % KCl and 67 mass % NaCl) in the amount of 2 % of metal mass. The first 4 melts are not treated with a complex modifier, melts 5-8 are modified with MK-1 /25/ at a temperature of 710 °C. The chemical compositions of all melts correspond to DSTU 2839-94. Heat treatment is carried out according to the T1 regime (aging at 210 °C), which also meets the requirements of DSTU 2839-94.

Table 1. Characteristics of experimental alloys.

Alloy number	Processing of melt MK-1, mass. (%)	Laser surface treatment	Test temperature (°C)
1	0	absent	20
2	0	absent	300
3	0	laser treated	20
4	0	laser treated	300
5	0.15	absent	20
6	0.15	absent	300
7	0.15	laser treated	20
8	0.15	laser treated	300

Fatigue test specimens had a plate shape with a cross-section of 2×6 mm. After aging, samples of alloys trunks 4, 5, 7, 8 are processed (on two side surfaces) with a QUANT 12 pulsed laser in melting mode (pulse duration 4 ms and wavelength 0.6943) with 30 % overlap of the tracks in the ambient atmosphere (treatment performed under supervision of Dr. V.V. Girzhon).

Subsequently, the samples are tested for fatigue on the basis of 10^7 cycles on the high-frequency stand IP-2 at a frequency of 18 kHz in accordance with the requirements of GOST 25.502-79 (under the supervision of Dr. O.E. Belsky). Samples of melts 1, 3, 5, 7 are tested at room temperature, melts 2, 4, 6, 8 at a temperature of 300 °C. According to the results of tests, curves are constructed in semi-logarithmic coordinates σ-logN.

Fractographic studies are carried out on samples destroyed after the fatigue test using a REM-106I scanning electron microscope in secondary electrons in the mode of accelerating voltage 30 kV.

Crack movement is analysed on samples that did not completely collapse and in which a crack began to develop during fatigue tests. For this, the end face is polished until a microcrack is detected, after which it is polished and etched with reagent (12.5 ml HCL, 25 ml HNO_3, 50 ml HCL, 12.5 ml H_2O). Identification of structural components and X-ray spectral microanalysis (EDX) is carried out on REM-106I in secondary electrons in the mode of accelerating voltage of 20 kV.

RESULTS AND DISCUSSION

For piston alloys, the optimal structure is a cellular α-solid solution of silicon in aluminium in the form of small dendrites and a eutectic containing lamellar silicon, located along the grain boundaries of the α-solid solution, thereby reliably blocking them. If the structure of the alloys contains crystals of primary silicon or complex intermetallic phases, it is recommended to obtain them in a compact form, with dimensions not exceeding 100 μm.

In this regard, to ensure the achievement of the desired structure, when developing the composition of the modifying complex MK-1, components are selected that have an active modifying effect on primary silicon crystals and complex intermetallic phases, reducing their size and changing the shape from a rough lamellar to a compact one, as well as refining the melt from non-metallic inclusions and dissolved gases.

The modifying complex includes: sodium carbonate Na_2CO_3, potassium carbonate K_2CO_3, ultrafine silicon carbide SiC, potassium hexafluorotitanate K_2TiF_6, potassium tetrafluoroborate KBF_4 and sulphur S. The choice of these components is based on the following. To reduce the rate of oxidation and sublimation of sulphur, as well as to grind the bubbles of gaseous sulphur, in order to increase the interface between the melt and the gas phase to ensure a higher degree of refining, Na_2CO_3 and K_2CO_3 are included in the modifying complex. The dissociation of these compounds in the melt with the release of carbon dioxide CO_2, which passes through the liquid metal bath, also helps to increase the level of refining. The presence of sodium and potassium compounds - known active modifiers of eutectic silicon, due to the amount being insufficient to completely modify the eutectic, ensures the production of eutectic silicon in the form of plates of small size and insignificant length. This is one of the main factors in obtaining a frame-type structure.

We include potassium hexafluorotitanate K_2TiF_6 in the modifying complex which, when dissociated, increases the efficiency of modifying the dendrites of the α-solid solution of silicon in aluminium, reducing the size of their cells and overall length. The presence of atomic titanium promotes the formation of additional crystallisation centres in the form of refractory, finely dispersed and uniformly distributed $TiAl_3$ intermetallic compounds. At the same time, the refining capacity of the complex is increased due to the passage of gaseous fluorine through the melt and the active binding of dissolved hydrogen.

The presence of ultradisperse silicon carbide (fraction 20 ... 40 nm) in the modifying complex ensures an increase in the number of crystallisation centres which, together with $TiAl_3$ intermetallic compounds during crystallisation, enhances the leading role of the α-solid solution of silicon in aluminium.

The presence of potassium tetrafluoroborate KBF_4 in the modifying complex, together with carbonates and fluorides, ensures the formation of a protective film on the surface of the melt, promotes the adsorption of slag inclusions and the simultaneous removal of hydrogen from the alloy, which forms a complex compound Al_2O_3-H_2 with aluminium oxide. In this regard, the presence of potassium tetrafluoroborate in combination with other elements is advisable, providing a high degree of melt refining, the required level of physical, mechanical and service properties, stabilisation of the structure with increasing temperature, which is very important for piston alloys.

On the destroyed samples of the secondary piston aluminium eutectic alloy, a typical picture of the fracture surface is observed under conditions of cyclic loads, which naturally changes depending on the temperature of the tests and the changes in the structure and surface condition of the samples.

Thus, the comparison of fractograms during the fatigue test at room temperature and at 300 °C reveals an increase in the size of the facets that change their orientation from grain-to-grain, Fig. 1, a, b. In the middle of each grain, the fracture trajectory resembles cleavage planes. As a result of the difference in grain orientation, part of the crack front propagates by a viscous mechanism, which leads to the formation of alternating terraces with viscous and brittle grooves.

Alloys 5 and 6 fuses are modified MK-1 and tested for fatigue at room temperature and at 300 °C. Typical fractograms of the fracture surfaces for these series of samples are shown in Fig. 1, c, d. A qualitative comparison makes it possible to assert that the fracture at higher temperatures occurs under the conditions of a decrease in its energy intensity, which is evidenced by an increase in the size of the structural components of the fracture.

The study of the movement of the crack along the structural components on undamaged samples, which are not

modified, reveals a tendency for the development of fracture in phases having a lamellar structure with sharp edges, Fig. 2.

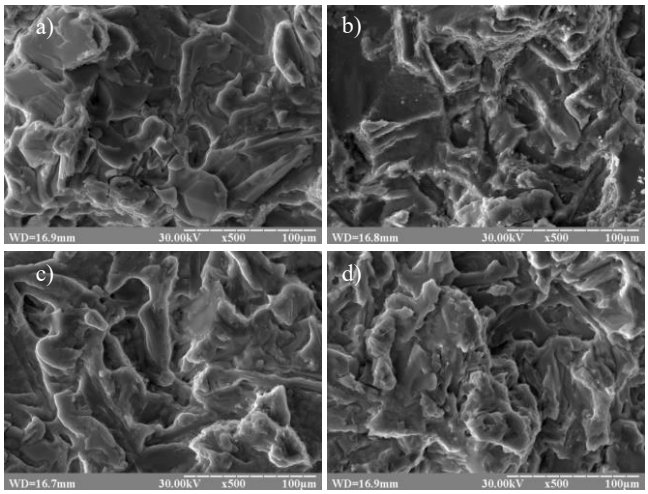

Figure 1. Fracture surfaces of AL25 secondary silumin (×500) with test temperatures: a) unmodified, 20 °C; b) unmodified, 300 °C; c) modified, 20 °C; d) modified, 300 °C.

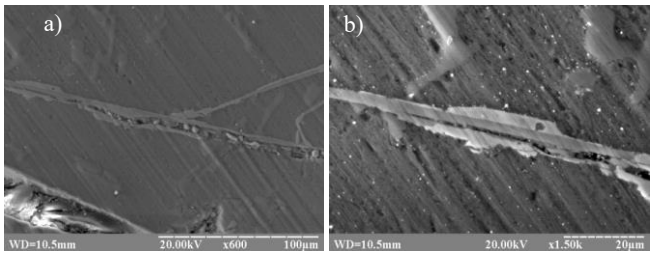

Figure 2. Crack propagation in unmodified AL25 alloy samples: a) ×600; b) ×1500.

Conducting EDX of the inclusions along which destruction took place (Fig. 3) indicates that inclusions of $Al_{15}(Fe,Mn,Ni,Cu)_3Si_2$, Al_3CuNi, $Al_{15}(Fe,Mn)_3Si_2$ phases had an unfavourable lamellar shape (Table 2). Also, the presence of secondary cracks is very often observed on specified inclusions, which also reduce the fatigue characteristics Fig. 4.

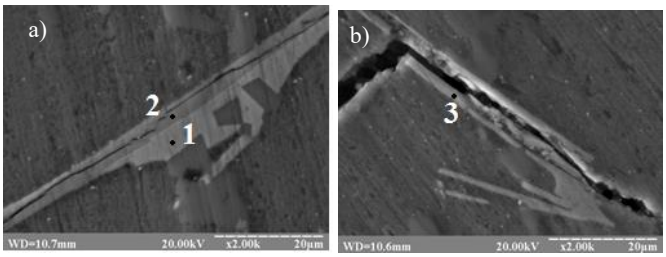

Figure 3. Locations of EDX (see Table 2).

Table 2. Chemical composition (at.%) in locations of AL25 alloy.

Loc.	Mg	Al	Si	Ti	Mn	Fe	Ni	Cu	Phase
1	0.22	68.86	4.14	-	1.2	3.13	18.99	3.44	$Al_{15}(Fe,Mn,Ni,Cu)_3Si_2$
2	0.22	68.93	7.25	0.08	13.47	8.6	0.74	0.69	$Al_{15}(Fe,Mn)_3Si_2$
3	0.02	53.49	0.42	0.15	0.05	0.197	27.97	17.7	Al_3CuNi

An increase in durability of silumins is possible in the case of using the MK-1 modifying complex which changes the morphology of secondary intermetallic phases and increases the energy intensity of the destruction process.

Examination of crack movement in modified samples did not reveal the passage of fracture along the structural components of lamellar shape. In most cases, the destruction takes place through compact inclusions which are classified as β-solid solution based on silicon and intermetallic of the type $Al_{15}(Fe,Mn,Ni,Cu)_3Si_2$ of the shape of hieroglyphs or are close to the hexagonal shape Fig. 5 (Table 3).

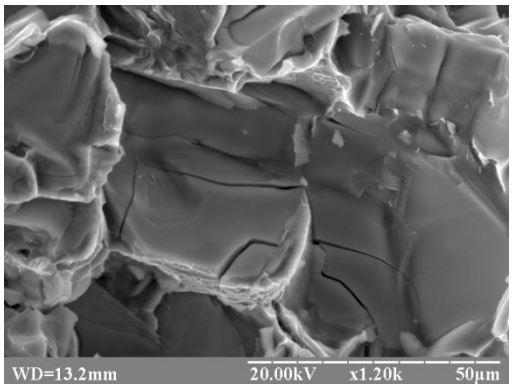

Figure 4. Secondary cracks in unmodified AL25 alloy, ×1200.

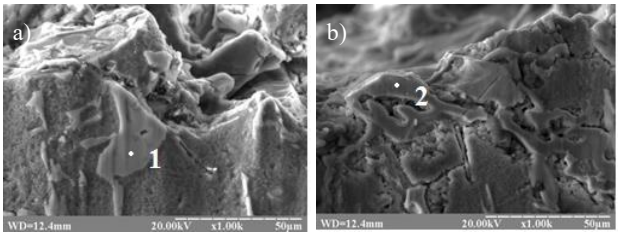

Figure 5. Locations of EDX of modified alloy: a) ×1000; b) ×1000.

Table 3. Results of EDX (at.%) at locations of destroyed samples.

Loc	Mg	Al	Si	Ti	Mn	Fe	Ni	Cu	Phase
1	-	2.4	97.60	-	-	-	-	-	Si
2	0.3	67.79	3.48	0.01	1.09	3.67	19.57	4.08	$Al_{15}(Fe,Mn,Ni,Cu)_3Si_2$

As a result of laser treatment in the remelting mode of the samples of alloys 3.4 and 7.8, the roughness of their surface increases sharply due to the formation of craters with a depth of 6-7 μm. The deterioration of quality of surface of the samples, as well as the appearance of tensile stresses due to the rapid cooling of the surface layer of molten metal, contributes to accelerated generation of microcracks on the molten surface of samples during the first load cycles Fig. 6. To reduce the effect of the geometric factor, the surface of samples after melting is polished to a roughness of Ra 032 with the removal of a layer of melted metal 30-50 μm thick from both sides of the samples.

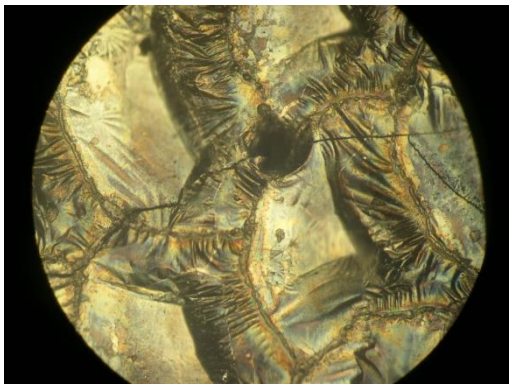

Figure 6. Surface of laser-treated sample with a crack after the first load cycles, ×500.

Typical fractograms of the fractured surface of the laser-treated layer of modified and unmodified samples are shown in Fig. 7. A comparison of the obtained fractograms did not reveal significant differences between the series of samples, and tests at elevated temperatures also have a slight effect. Such minor differences are due to the formation of a homogeneous solid solution after laser treatment, which does not change its state even when heated to 300 °C.

Since crack initiation and the destruction of sample during cyclic tests begins from the surface, the laser-treated layer is the first to resist fatigue crack propagation. As with all cyclic fractures, it is characterised by initial movement of the crack at an angle of 45° to the surface, which is clearly visible in Fig. 7, a, b. Fatigue crack development is characterised by a change in the orientation of the main fracture plane in each grain from one or two shear planes to many parallel terraces separated by longitudinal ridges. These terraces are perpendicular to the direction of maximal stress. Also clearly visible are details of viscous fatigue grooves which have a fibrous character with a clear propagation front, Fig. 8.

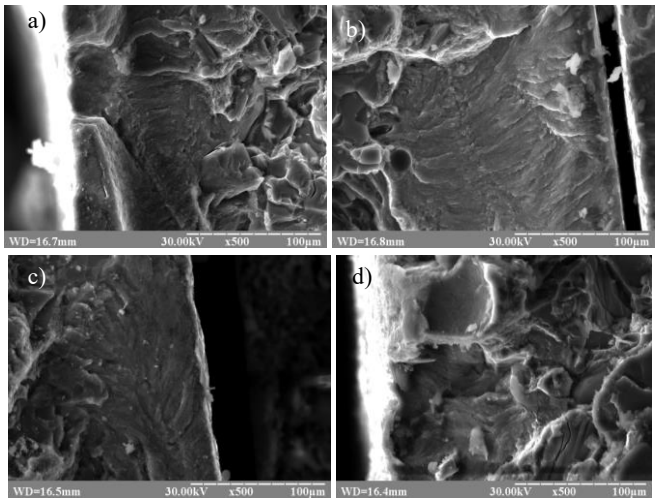

Figure 7. Fracture surfaces of the laser-treated layer in modified and unmodified samples, ×500: a), b) without modification; c), d) with modification; a), c) at 20 °C; b), d) at 300 °C.

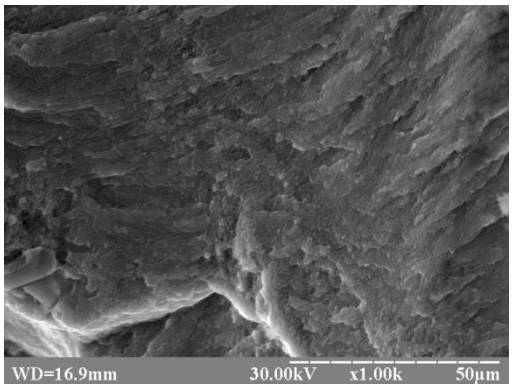

Figure 8. Fracture surface of laser-treated AL25 alloy sample.

A comparison of fractograms of the main non-laser-treated material did not reveal significant differences between samples of alloys 5, 6. The nature of the destruction remains typical for cyclic tests, the difference between samples fractured at room temperature and at 300 °C is characterised by an increase in size of structural components of the fracture.

A comparison of the results of fatigue strength tests of all melts show that the highest fatigue characteristics have samples of alloy 5, only treated with the modifying complex Fig. 9. This is caused by a change in morphology of intermetallic inclusions (there is a change from plate and needle shape to the type of Chinese characters or hexagon) Fig. 10, which increases the energy intensity of the movement of cracks in the material.

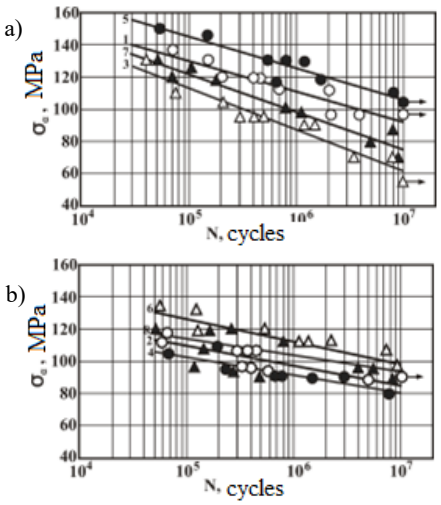

Figure 9. Fatigue curves of secondary piston silumin AL25: a) at 20 °C; b) at 300 °C.

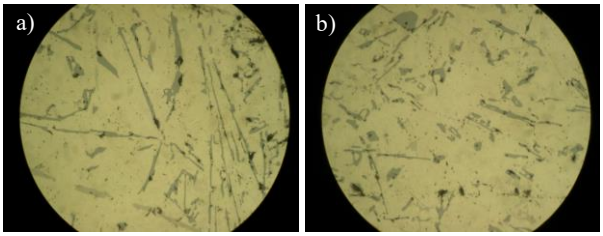

Figure 10. Microstructure of AL25 alloy, ×500: a) without modification (alloy 1); b) treatment with 0.15 % MK-1 (alloy 5).

A typical structure for alloys 1-4 is the presence of large lamellar and needle-like inclusions with a slight cross-section in thickness, Fig. 10a. The average shape parameter for them is 58.4, which indicates the large length of these inclusions. In addition, the ends of plates have a small radius of rounding which can serve as the centre of crack initiation. This leads to the fact that unmodified samples have approximately 15-20 MPa lower fatigue strength indicators compared to the modified ones.

Increasing the test temperature to 300 °C, Fig. 9b, slightly reduces the fatigue strength of samples which can be explained by growth of diffusion processes and the increase in the mobility of atoms which reduces the energy intensity of the destruction process. Also, the angle of inclination of the fatigue curves is also reduced by almost half, and the effect of modification is expressed much more. Thus, the difference between modified and unmodified samples increases to 20-25 MPa.

All laser-treated samples show lower cyclic strength than untreated ones. This behaviour can be caused by significant fragility and roughness of the surface of samples which significantly improves the conditions for crack initiation. Thus, during laser treatment, it is necessary to pay attention to the

treated surface, since the increase in fragility and roughness significantly reduces the durability of the material.

CONCLUSIONS

A qualitative comparison of fractograms of fractured surfaces of AL25 secondary piston silumin samples after cyclic fatigue testing is conducted. An increase in the size of structural component fractures with increasing temperature and a decrease with the introduction of the modifying complex are revealed.

It is established that in samples without modification, the crack moves along lamellar or needle-shaped intermetallic, from which the formation of secondary cracks is possible, further reducing the properties of the material.

The introduction of a modifying complex significantly increases the cyclic strength of samples and changes the paths of crack movement along more energy-intensive structural components.

Laser treatment reduces the fatigue strength of samples due to the presence of a developed surface.

REFERENCES

1. Mucci, G., Bernhard, J., Baumgartner, J., Frendo, F. (2021), *Fatigue assessment of laser beam and friction stir welded joints made of aluminium*, Weld. World, 65: 611-621. doi: 10.1007/s40194-020-01045-4
2. Mumović, M., Šibalić, N., Bajić., D., Vukčević, M. (2021), *Numerical analysis of welding sequence influencing the quality of an AA6060-T4 alloy lap joint*, Struct. Integr. Life, 21(2): 123-130.
3. Olohunde, S.T., Hafizi, A.M., Jamaliah, I., et al. (2019), *Corrosion resistance of aluminium-silicon hypereutectic alloy from scrap metal*, J Bio- Tribo-Corros. 5: 41. doi: 10.1007/s40735-019-0224-x
4. Girish, G., Gopi, G. (2023), *Improving the mechanical and corrosion properties of aerospace-grade AA7075 through microstructural modification using low-temperature friction stir processing*, Bull. Mater. Sci. 46: 217. doi: 10.1007/s12034-023-03054-7
5. Wang, L., Shivkumar, S. (1995), *Strontium modification of aluminium alloy castings in the expendable pattern casting process*, J Mater. Sci. 30: 1584-1594. doi: 10.1007/BF00375269
6. Girinath, B., Siva Shanmugam, N., Sankaranarayanasamy, K. (2019), *Investigation on the effect of torch angle on the formability of AA5052 CMT weldments*, Trans. Ind. Inst. Met. 72: 1551-1555. doi: 10.1007/s12666-019-01633-z
7. Srivastava, M.C., Lohne, O. (2016), *Effects of heat treatment on the microstructure and mechanical properties of ductile AlSi9MgMn die castings*, Int. J Metalcast. 10: 556-565. doi: 10.1007/s40962-016-0049-z
8. Yadav, P.K., Patel, S.K., Singh, V.P. et al. (2021), *Effect of different reinforced metal-matrix composites on mechanical and fracture behaviour of aluminium piston alloy*, J Bio- Tribo-Corros. 7: 54. doi: 10.1007/s40735-021-00478-8
9. Saleh, A.A. (2020), *Joining of AA2014 and AA5059 dissimilar aluminium alloys by friction stir welding*, Struct. Integr. Life, 20(2): 99-102.
10. Temesi, T., Czigany, T. (2022), *Laser-joined aluminium-polypropylene sheets: the effect of the surface preparation of aluminium*, Int. J Adv. Manuf. Technol. 121: 6907-6920. doi: 10.1007/s00170-022-09790-0
11. Uthirapathi, E., Chinnamuthu, S., Kaliyamoorthi, N. (2024), *An examination on dry sliding wear behaviour of AA7075 aluminium alloy modified with FA/Cu electro-discharge coating*, J Bio-Tribo-Corros. 10: 25. doi: 10.1007/s40735-024-00828-2
12. Mukherjee, M., Kundu, J., Shome, M. (2022), *Effect of processing parameters on the interface characteristics and joint strengths of aluminium-on-steel lap joints produced using conduction mode laser welding*, Weld. World, 66(12): 2461-2482. doi: 10.1007/s40194-022-01392-4
13. Millán, L., Bokuchava, G., Hidalgo, J.I., et al. (2021), *Study of microscopic residual stresses in an extruded aluminium alloy sample after thermal treatment*, J Surf. Invest. 15: 763-767. doi: 10.1134/S1027451021040145
14. Poole, W.J., Sæter, J.A., Skjervold, S., Waterloo, G. (2000), *A model for predicting the effect of deformation after solution treatment on the subsequent artificial aging behavior of AA7030 and AA7108 alloys*, Metall. Mater. Trans. A, 31: 2327-2338. doi: 10.1007/s11661-000-0148-5
15. Kim, S.W., Hao, H. (2003), *Microstructure and fatigue characteristics of direct chill cast and electromagnetic cast 2024 Al alloy ingots*, Metall. Mater. Trans. A, 34: 1537-1543. doi: 10.1007/s11661-003-0265-z
16. Tan, Y., Zhao, H., Xu, Q. (2024), *Numerical simulation of solidified microstructure of ternary Al-Si-Mg alloy using an improved cellular automaton method*, Sci. China Mater. 67: 1150-1159. doi: 10.1007/s40843-023-2706-x
17. Ho, C.S., Mohd Nor, M.K. (2021), *An experimental investigation on the deformation behaviour of recycled aluminium alloy AA6061 undergoing finite strain deformation*, Met. Mater. Int. 27: 4967-4983. doi: 10.1007/s12540-020-00858-8
18. Petrović, Z., Burzić, Z., Perković, S., et al. (2021), *Corrosion effect on mechanical properties of aluminium alloys 2024-T351 and 7075-T651*, Struct. Integr. Life, 21(2): 197-200.
19. Lee, C-D. (2022), *Effect of stress ratio on fatigue life of A356 aluminium casting alloys*, J Mater. Eng. Perform. 31: 1066-1076. doi: 10.1007/s11665-021-06297-9
20. Srinivasa Rao, K., Naga Raju, P., Reddy, G.M., Prasad Rao, K. (2010), *Microstructure and impression creep of age hardenable AA2219 aluminium alloy modified by Sc, Mg and Zr additions*, Trans. Ind. Inst. Met. 63: 379-384. doi: 10.1007/s12666-010-0051-8
21. Patel, A., Nastac, L. (2014), *Mathematical modeling of microshrinkage formation during solidification of A356 castings*, Int. J Metalcast. 8: 21-27. doi: 10.1007/BF03355568
22. Kunisetti, P., Prasad, B.S., Chandra Mouli, K.V.V.N.R. (2024), *Influence of varied laser density on sintering processing parameters, mechanical properties, and microstructural characteristics of DMLS-printed AlSi10Mg materials: A comparative experimental study*, Trans. Ind. Inst. Met. 77: 523-531. doi: 10.1007/s12666-023-03120-y
23. Kraedegh, A., Li, W., Sedmak, A., et al. (2017), *Simulation of fatigue crack growth in A2024-T351 T-welded joint*, Struct. Integr. Life, 17(1): 3-6.
24. Lemmadi, F.Z., Chala, A., Belahssen, O., Benramache, S. (2016), *Effect of heat treatments on structural, microstructural and mechanical properties of Al 2017 alloy*, Phys. Metals Metallogr. 117: 83-88. doi: 10.1134/S0031918X16010099
25. Loza, K.M., Mityaev, O.A., Volchok, I.P. (2009), *Modifying complex for aluminium alloys*, Patent UA no. u200905914 (in Ukrainian)